Gluon contribution to hadronic J/ψ production

M. Glück
Institut für Physik, Universität Mainz, 6500 Mainz, West Germany

J. F. Owens
Department of Physics, Florida State University, Tallahassee, Florida 32306

E. Reya
Institut für Physik, Universität Mainz, 6500 Mainz, West Germany
and Department of Physics, Florida State University, Tallahassee, Florida 32306

(Received 29 August 1977)

Using the recent CERN and Fermilab measurements for J/ψ production by $\pi^{\pm}$, $K^{\pm}$, p, and $\bar{p}$ beams we show, within the framework of quantum chromodynamics, that only a *combined* version of light-quark $q\bar{q} \to c\bar{c}$ fusion *and* gluon $gg \to c\bar{c}$ fusion mechanisms can account for the various total-cross-section beam ratios as well as for the observed x_F distributions.

I. INTRODUCTION

Since the discovery of J/ψ signals in pBe scattering[1] there have been several theoretical attempts to understand the origin of these events within the framework of the Drell-Yan[2] quark-fusion model. So far the following mechanisms have been suggested:

(i) Fusion of light- ($q = u, d, s$) quark-antiquark pairs[3,4] to annihilate into a J/ψ as shown in Fig. 1. The coupling of the $q\bar{q}$ system to the J/ψ is very small (Zweig's rule), of the order $g_{q\bar{q}\psi}{}^2/4\pi \simeq 10^{-5}$. This mechanism is therefore of little significance and yields a negligible contribution to the total cross section.

(ii) Fusion of heavy charmed quarks[3-5] to produce the J/ψ system as shown in Fig. 2. Here the coupling is not small, $g_{c\bar{c}\psi}{}^2/4\pi \simeq 0.2$–$0.5$, but the very small charmed sea[6,7] enters the cross section *quadratically* so that this mechanism also yields only a negligible contribution to the total cross section. In Refs. 3–5 a non-negligible contribution was achieved by postulating an unusually large *and* flat sea. This large charmed sea does not seem to be compatible with recent data[8] on $\sigma^{\bar{\nu}}/\sigma^{\nu}$, $\langle y \rangle^{\bar{\nu}}$ and on μp deep-inelastic scattering[9] as pointed out in Ref. 10. Furthermore, the color suppression factor was *not* incorporated in these calculations. In addition, the absence of extra muons[11] produced in association with the J/ψ suggests that it is not made by $c\bar{c}$ annihilation.

(iii) Fusion of ordinary light SU(3) u, d, s quarks to produce a highly virtual gluon which then decays into a $c\bar{c}$ pair as shown in Fig. 3. The production of a particular state, e.g., J/ψ, depends on the dynamical details of the strong-interaction mechanism by which the color-octet $c\bar{c}$ configuration rearranges itself, by soft-gluon emmission, into a definite outgoing color-neutral $c\bar{c}$ state. This mechanism, suggested by Fritzsch,[12] is potentially of great importance since the coupling constant is not too small and the sea ($\bar{q}$) now enters the cross section only *linearly*. This model makes definite predictions for J/ψ production ratios by different beams. Specifically, it predicts[12] very large values for $\bar{p}/p \equiv \sigma(\bar{p}N \to J/\psi + X)/\sigma(pN \to J/\psi + X)$ in contrast to the much smaller (by one order of magnitude) experimental value.[13] This strongly indicates that J/ψ is not made by $q\bar{q}$ annihilation alone. We therefore suggest the following further significant mechanism of the same kind:

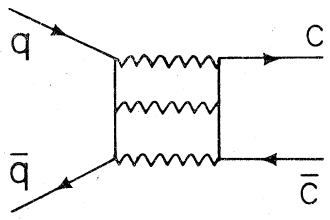

FIG. 1. Production of J/ψ through fusion of ordinary $q = u, d, s$ quarks.

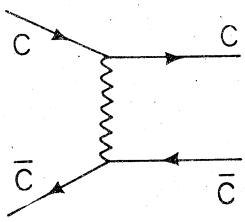

FIG. 2. Production of J/ψ through fusion of charmed quarks.

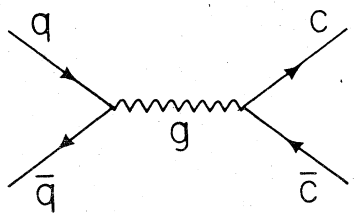

FIG. 3. Production of ψ states through fusion of ordinary u, d, s quarks into a *single* colored gluon with subsequent decay into a $c\bar{c}$ pair, where the emission of soft gluons is implicitly implied in order to form colorless $C=\pm 1$ states.

(iv) Fusion of two gluons to produce a virtual gluon which then decays into a $c\bar{c}$ state as discussed in (iii). The corresponding graph in Fig. 4(a) is not gauge invariant and the graphs of Figs. 4(b) and 4(c) are needed in addition. These latter two diagrams resemble the Einhorn-Ellis[14] graphs which have been studied[14,15] in connection with the production of $C=+1$ states (η_c or p-wave χ states) which can also decay into a J/ψ by emitting a soft photon. However, the contribution of this cascade mechanism to J/ψ production, appears to be suppressed by a factor α/α_s (soft) $\simeq 10^{-1}$–10^{-2} relative to the direct J/ψ production from a $c\bar{c}$ pair via soft-gluon emission. It should be emphasized that the Einhorn-Ellis graphs of Figs. 4(b) and 4(c) are *not* gauge invariant in quantum chromodynamics (QCD).

The mechanism (iv) suggested here yields $\bar{p}/p = 1$. Since experimentally[13] $\bar{p}/p > 1$ (but *not* $\gg 1$) it is obvious that J/ψ is produced through a *combination* of mechanisms (iii) and (iv). The relative weight of these contributions is fixed by the quark and gluon content of the hadrons and by the ratio of the total cross sections $\sigma(q\bar{q} \to c\bar{c})/\sigma(gg \to c\bar{c})$ at c.m. energies of about[12] 3.1–3.7 GeV. In Sec. II we present our calculations for these cross sections and explain our gluon and quark input distributions. We then proceed, in Sec. III, to apply these results to x_F distributions as well as to various measured total cross sections and cross-section beam ratios for J/ψ production. The conclusions are presented in Sec. IV and some details of the gluon-gluon cross section calculation are given in the Appendix.

II. CALCULATION OF THE CROSS SECTIONS

Adopting the local duality approach of Ref. 12 one estimates the cross section for producing any $c\bar{c}$ state below charm threshold through fusion of quarks q in the incoming hadron A with antiquarks $\bar{q}$ in the target B (and vice versa) to be proportional to

$$\frac{d\sigma_{q\bar{q}}^{AB}}{dx_F} = \sum_{q=u,d,s} \int_{4m_c^2}^{4m'^2} dQ^2 \sigma^{q\bar{q}\to c\bar{c}}(Q^2) \frac{1}{Q^2} \frac{x_A x_B}{x_A + x_B} \times [q^A(x_A, Q^2)\bar{q}^B(x_B, Q^2) + q \leftrightarrow \bar{q}], \tag{1}$$

where $m_c \simeq 1.5$ GeV, $m' \simeq 1.85$ GeV, and $x_{A,B} = \frac{1}{2}[\pm x_F + (x_F^2 + 4Q^2/s)^{1/2}]$ with $s = (p_A + p_B)^2$. The longitudinal momentum fraction of the produced $c\bar{c}$ state is given by $x_F = x_A - x_B$, and q^A stands for the distribution of quarks in A. Similarly the cross section stemming from the gluon-gluon annihilation $gg \to c\bar{c}$ reads

$$\frac{d\sigma_{gg}^{AB}}{dx_F} = \int_{4m_c^2}^{4m'^2} dQ^2 \sigma^{gg\to c\bar{c}}(Q^2) \frac{1}{Q^2} \frac{x_A x_B}{x_A + x_B} \times G^A(x_A, Q^2) G^B(x_B, Q^2), \tag{2}$$

where G^A is the distribution of gluons in A. The

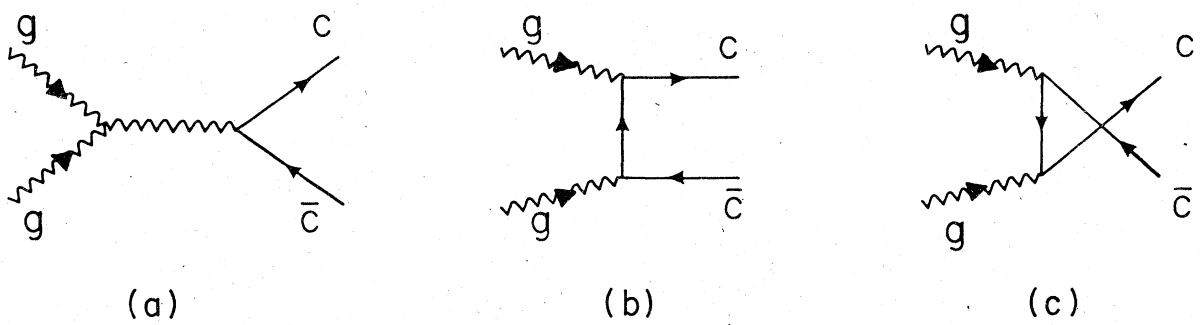

FIG. 4. (a) Production of ψ states through fusion of gluons into a single colored gluon with subsequent decay into a $c\bar{c}$ pair where soft-gluon emission is implied to form physical colorless states as in Fig. 3. (b) and (c) Gauge-invariance partners of Fig. 4(a).

total x_F distribution for a produced $c\bar{c}$ state is then the sum of Eqs. (1) and (2), i.e., $d\sigma^{AB}/dx_F \equiv d(\sigma_{q\bar{q}}^{AB} + \sigma_{gg}^{AB})/dx_F$ from which we obtain the total $c\bar{c}$ production cross section by integrating over $0 \leq x_F \leq 1 - Q^2/s$ with the lower limit dictated by experimental cuts.

The relevant cross section for the annihilation subprocesses in Fig. 3 is given by

$$\sigma^{q\bar{q}\to c\bar{c}} = \frac{2}{9}\frac{4\pi\alpha_s^{\,2}}{3Q^2}(1+\tfrac{1}{2}\gamma)(1-\gamma)^{1/2}, \tag{3}$$

where $\gamma = 4m_c^{\,2}/Q^2$. The factor $\frac{2}{9}$ is the familiar QCD color factor and $\alpha_s = 12\pi/25\ \ln(Q^2/\Lambda^2)$ with $\Lambda \simeq 0.5$ GeV. For the gluon-gluon fusion process of Fig. 4 one obtains, as further discussed in the Appendix,

$$\sigma^{gg\to c\bar{c}} = \frac{\pi\alpha_s^{\,2}}{3Q^2}\left((1+\gamma+\tfrac{1}{16}\gamma^2)\ln\frac{1+(1-\gamma)^{1/2}}{1-(1-\gamma)^{1/2}} - (\tfrac{7}{4}+\tfrac{31}{16}\gamma)(1-\gamma)^{1/2}\right). \tag{4}$$

The QCD quark and gluon distributions used in the calculations will be taken from Ref. 16, where they were uniquely calculated using renormalization group techniques based on the dynamical assumption that at low resolution energies hadrons consist of valence quarks only. For the case of the pion the valence distribution has to be specified at $Q^2 = Q_0^{\,2} = 3$ GeV^2. With this input, together with the above mentioned dynamical assumption, the valence, sea, and gluon terms are completely specified for arbitrary Q^2 values. For the nucleon case a similar approach is used except that deep-inelastic lepton-scattering data are used as input at $Q^2 = Q_0^{\,2}$. For the purpose of numerical calculations the results for the various distributions have been parametrized in convenient forms which accurately reproduce the distributions in the region $x \gtrsim 0.03$ and $3.0 \lesssim Q^2 \lesssim 250$ GeV^2. For $x \lesssim 0.03$ these parametrizations somewhat underestimate the sharply peaked dynamically calculated sea and gluon distributions, thereby leading to an apparent contradiction with the momentum sum rule. However, for the calculations presented here the very small x region is not probed.

One of the pionic valence distributions used in Ref. 16 is characterized by $xv^\pi(x) \neq 0$ at $x = 1$ as advocated by Feynman and Field.[17] Since the cross section for J/ψ production with $\pi^\pm$ beams in the region $x_F \gtrsim 0.4$ is sensitive to the behavior of $xv^\pi(x)$ as $x \to 1$, we will also use dynamically[16] calculated π distributions for which $xv^\pi(x) = 0$ at $x = 1$. The QCD predictions for the latter ones at $Q^2 = Q_0^{\,2} = 3$ GeV^2 and for $x \gtrsim 0.03$ can be parametrized as

$$\begin{aligned} xv^\pi(x,Q_0^{\,2}) &= 0.75\sqrt{x}\,(1-x), \\ x\xi^\pi(x,Q_0^{\,2}) &= 0.018(1-x)^{3.5} + 0.007(1-x)^7 \\ &\quad + 0.091(1-x)^{11}, \\ xG^\pi(x,Q_0^{\,2}) &= 0.309(1-x)^{2.5} + 0.715(1-x)^7 \\ &\quad + 1.511(1-x)^{11}, \end{aligned} \tag{5}$$

where the QCD Q^2 evolution for the valence (v^π), sea (ξ^π), and gluon (G^π) distribution is approximately given by Eq. (A5) of Ref. 16. For our present purpose, however, this additional Q^2 dependence of parton distributions is almost negligible.

For comparison we also will use a typical representative parametrization of the *naive* quark-parton model, i.e., $q^A(x_A, Q^2) \equiv q^A(x_A)$ and $G^A(x_A, Q^2) \equiv G^A(x_A)$. For nucleons we use the one of Barger and Phillips[18] combined with a gluon dictated by counting rules,

$$xG^N(x) = 3(1-x)^5 \tag{6}$$

and, similarly, for the π distributions we take[19]

$$\begin{aligned} xv^\pi &= 0.75\sqrt{x}\,(1-x), \\ x\xi^\pi &= 0.1(1-x)^5, \\ xG^\pi &= 2(1-x)^3. \end{aligned} \tag{7}$$

Assuming local SU(3) symmetry[19] we take the parton and gluon distributions in kaons to be the same as in pions. This should provide a reasonable first-order approximation to the scarce $K^\pm$-beam data[13] available.

III. RESULTS

A. x_F distributions

The recent CERN-Omega J/ψ production experiment[13] using 39.5-GeV/c incident $\pi^\pm$ beams on copper provides a very sensitive test for the quark and gluon distributions in the pion. In Fig. 5 we compare our predictions for $d\sigma/dx_F$ with these (unnormalized) data which strongly favor a Farrar-type pionic valence distribution, i.e., $xv^\pi(x) \sim (1-x)$ as $x \to 1$, as shown by the solid curves. The predictions using a Feynman-Field–type valence input (dashed curves) are clearly incompatible with the large-x_F dependence of J/ψ production, this region of x_F being particularly sensitive to the behavior of $xv^\pi(x)$ as $x \to 1$. Thus, for dynamical QCD as well as naive parton-model distributions, we will use only the Farrar-type pionic distributions hereafter, as given by Eq. (5) or (7). Figure 6 shows the individual contributions to $d\sigma/dx_F$ stemming from ordinary light-quark $q\bar{q}$ fusion and gluon gg fusion as given by Eqs. (1) and (2), respectively. Although the inclusion of the $gg \to c\bar{c}$ subprocess improves the agreement with the data,

by increasing the otherwise too flat $q\bar{q}$ cross section at small x_F, its total contribution is rather small since for $s = 76$ GeV^2 the dominant contribution in Eq. (2) comes from a region where $x_A, x_B \gtrsim 0.2$.

Our predictions for the high-energy Fermilab-Chicago-Princeton data[20] using π^+, π^-, and p beams are shown in Fig. 7 where the (parameter-free) dynamical QCD parton distributions have been used in Fig. 7(a) [with the pionic densities given by Eq. (5)], and Fig. 7(b) results from using the naive quark-parton-model distributions of Barger and Phillips[18] supplemented by Eqs. (6) and (7). Here the gluon-gluon contribution is required in order to reproduce the observed x_F dependence of the data, in contrast to the claims of Ref. 21. The $q\bar{q}$ fusion alone can obviously not account for the data, yielding too flat an x_F distribution in each instance. It should be noted that the predictions are, of course, the same for both the π^+ and π^- beams. The overall normalization is obviously a free parameter since we cannot reliably calculate how the color-octet $c\bar{c}$ configuration rearranges itself by soft-gluon emission into an observable color-neutral $c\bar{c}$ resonance. The theoretical predictions of Eqs. (1) and (2) shown in Fig. 7 have been calculated using a $J/\psi \to \mu^+\mu^-$ branching ratio $B = 0.07$ and by dividing by factors of 2 and 8 for Figs. 7(a) and 7(b), respectively. This is in approximate agreement with the naive expectation[12] that the cross section for J/ψ production should be smaller than the Q^2-integrated cross sections of Eqs. (1) and (2) by roughly a factor 2...7 according to an equal sharing between η_c and J/ψ or an equal sharing between η_c, J/ψ, ψ' and the four p states P_c/χ.

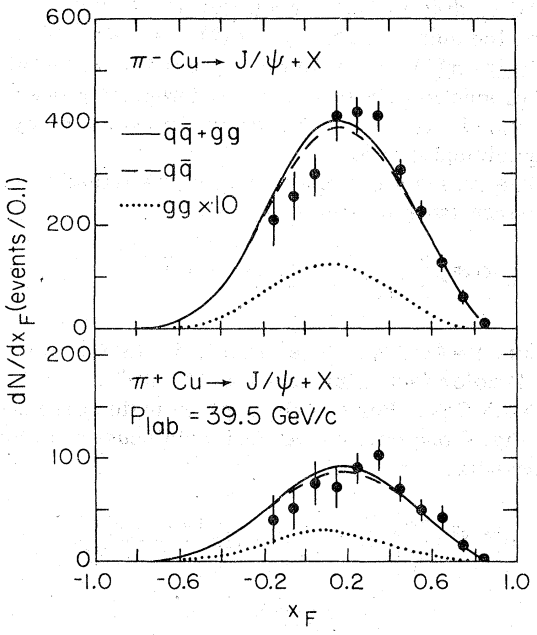

FIG. 6. Individual contributions from the light-quark $q\bar{q}$ and gluon-gluon (gg) fusion processes using Farrar-type QCD π distributions. The solid curves and the data are the same as in Fig. 5.

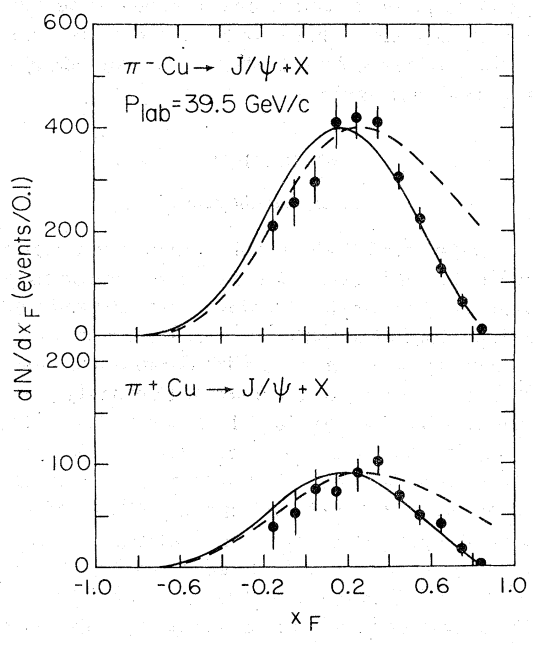

FIG. 5. Comparison of the (unnormalized) CERN data (Ref. 13) with the predictions of the combined $q\bar{q}$ and gg fusion model, Eqs. (1) *and* (2), using dynamically calculated (Ref. 16) QCD quark and gluon distributions. The solid curves correspond to using the Farrar-type π distributions of Eq. (5), whereas the dashed curves result from using a pionic Field-Feynman– type valence input (Ref. 16) $xv^{\pi}(x, Q_0^2) = \frac{3}{8}\sqrt{x}\,(\frac{5}{3} - x)$.

B. Total cross sections

Figure 8 shows our predictions for the ratios of the various total J/ψ production cross sections using p, $\bar{p}$, $\pi^{\pm}$, and $K^{\pm}$ beams. In order to demonstrate the dependence on different parton distributions we show the predictions for the same two extreme sets of densities used in Fig. 7, namely for the QCD (solid curves) and naive parton model (dashed curves) distributions. It is clear from Fig. 8 that the $q\bar{q}$ fusion model alone is not capable of accounting for the data. The additional contribution from gluon-gluon (gg) fusion is not only required by the low-energy CERN data[13] but also by the high-energy Fermilab measurement[20] of p/π^+. The latter one clearly demonstrates the essential role of the gluon-gluon fusion mechanism and that only the combination of $q\bar{q}$ *and* gg

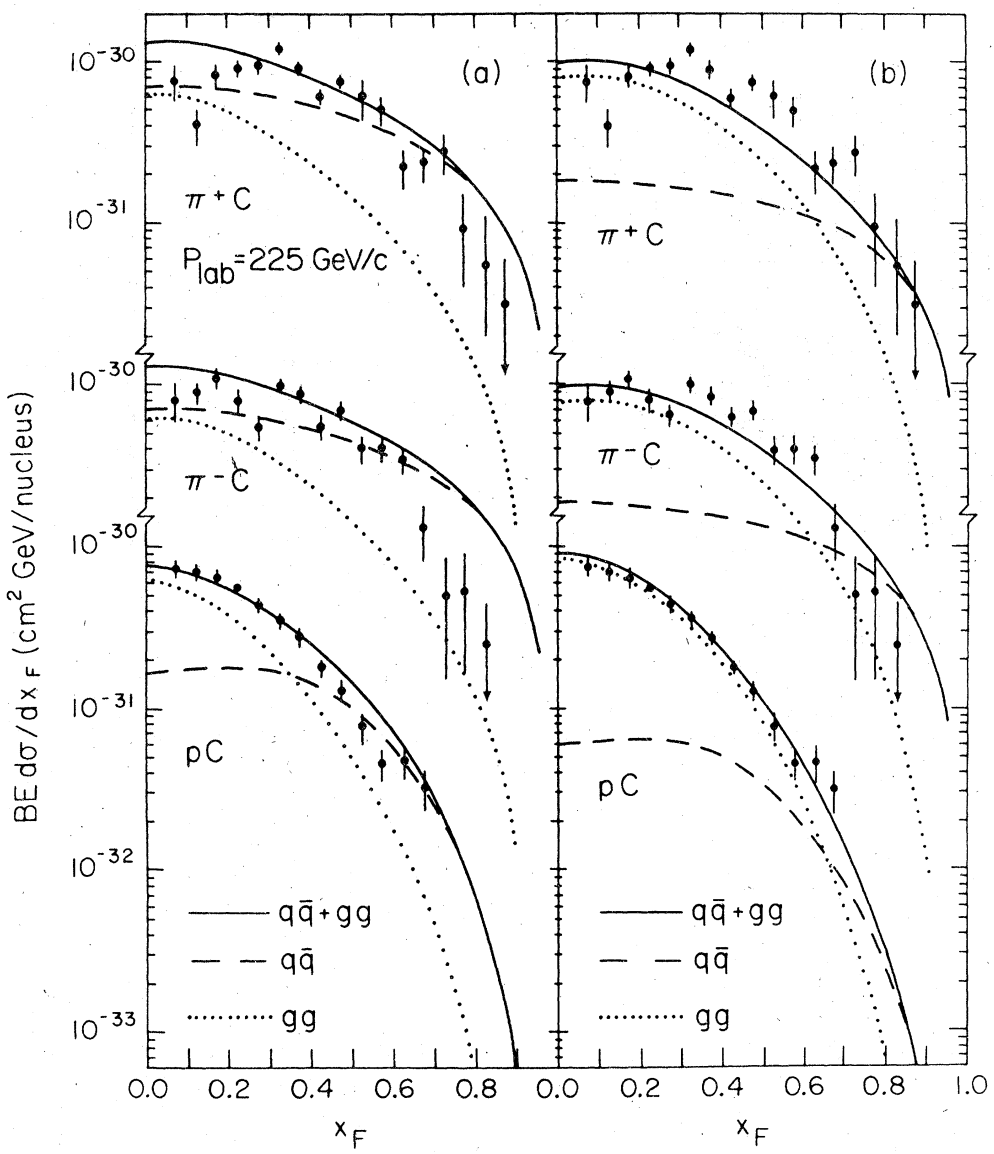

FIG. 7. Comparison of experimental x_F distributions (Ref. 20) for producing $\mu^+\mu^-$ pairs in the mass interval $\sqrt{Q^2}$ = 2.7–3.5 GeV using $\pi^\pm$ and p beams [$E = (m_\psi^2 + s x_F^2/4)^{1/2}$] with the predictions of Eq. (1) and (2) using (a) dynamical QCD nucleonic and pionic, Eq. (5), parton distributions (Ref. 16); (b) naive quark-parton distributions of Barger and Phillips (Ref. 18) supplemented by Eqs. (6) and (7). The π^+ and π^- predictions are identical.

fusion can correctly reproduce the observed strong energy dependence of p/π^+. It will be particularly interesting to see whether the forthcoming CERN experiment using a high-energy $\bar{p}$ beam will observe a similar strong increase of $p/\bar{p}$, and consequently an almost energy-independent $\bar{p}/\pi^-$ ratio, in contrast to the predictions of the pure $q\bar{q}$ fusion model.[12] The $q\bar{q}$ and/or gg fusion model (trivially) predicts $\pi^+/\pi^- = 1$ independent of energy. This is in good agreement with experiment, i.e., $\pi^+/\pi^- = 0.87 \pm 0.14$ and 0.87 ± 0.12 at low[13] and high[20] energies, respectively, confirming the $q\bar{q}$ and gg fusion mechanism for explaining hadronic J/ψ production.

In Fig. 9 the energy dependence of $Bd\sigma/dy\,|_{y=0}$ is shown for both the QCD and the naive parton-model distributions. The solid and dotted curves have been calculated using the dynamical QCD distributions of Ref. 16 while the dashed line was calculated using the naive parton-model distributions of Ref. 18 together with Eq. (6). The $q\bar{q}$ curve for the naive parton-model distributions has

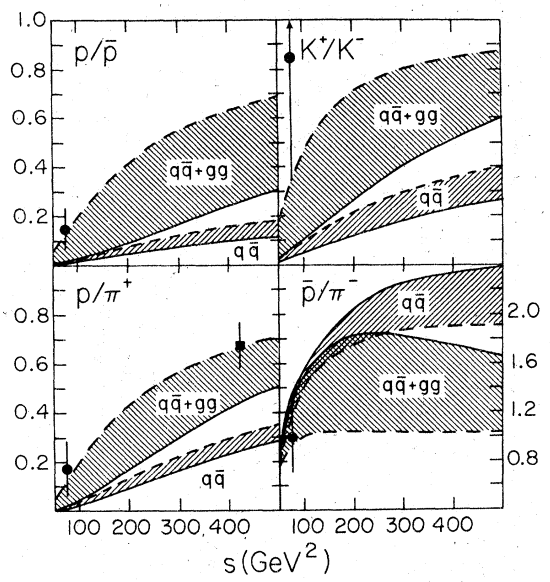

FIG. 8. Predictions for the beam ratios of total J/ψ production cross section using incident p, $\bar{p}$, $\pi^{\pm}$, and $K^{\pm}$ beams. The solid curves correspond to the dynamical QCD distributions as used in Fig. 7(a), and the dashed curves refer to the naive parton model densities as in Fig. 7(b). The data ($x_F > 0$) are taken from Refs. 13 and 20.

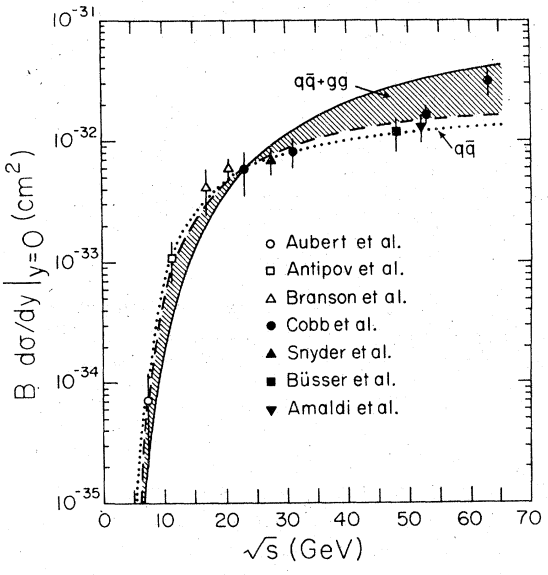

FIG. 9. The energy dependence of $Bd\sigma/dy$ for $pN \to (J/\psi \to \mu^+\mu^-) + X$ at center-of-mass rapidity $y = 0$. The solid and dotted curves correspond to the QCD parton distributions as used in Fig. 7(a) and the dashed curve refers to the naive parton and gluon distributions used in Fig. 7(b). The latter ones yield a result for the $q\bar{q}$ mechanism alone which is similar to the dotted curve. The data were taken from Refs. 1 and 22–28.

been omitted for clarity, since it is very similar to the QCD distribution result shown by the dotted line. Each curve has been separately normalized to the point at $\sqrt{s} = 23$ GeV to facilitate the comparison of the *shapes* of the different predictions. The shaded area again represents the region corresponding to the two choices of distributions used in Figs. 7 and 8. The rapid initial rise and subsequent slow increase observed in the data is well described either by the $q\bar{q}+gg$ shaded area or the $q\bar{q}$ curve. This shows that in the present energy range the energy dependence of the J/ψ production cross section is not an overly sensitive probe of the gluon-gluon fusion mechanism. However, at higher energies ($\sqrt{s} \gtrsim 200$ GeV) the difference between the $q\bar{q}$ and $q\bar{q}+gg$ curves becomes greater. Therefore, if the rising trend shown by the present (CERN ISR) data continues this could be taken as another indication of the importance of the gluon-gluon fusion mechanism.

C. Discussion

In Figs. 7, 8, and 9 the predictions corresponding to two sets of quark and gluon distributions have been shown. In each case, the data seem to favor slightly the use of the counting rule gluon distribution [Fig. 7(b) and dashed curves in Figs. 8 and 9]. The difference is due to the fact that the dynamically calculated QCD gluon distribution is concentrated at small x and has a very steep slope in this region, whereas the counting-rule gluon distribution is much flatter, giving a larger fraction of hard gluons. At a fixed value of $\sqrt{s}$ this results in a larger $gg/q\bar{q}$ ratio in the total and differential cross section. This increased gluon contribution improves the predictions for the x_F dependence and total-cross-section beam ratios. The flatter x slope also yields a more moderate increase with energy for $Bd\sigma/dy\,|_{y=0}$.

This behavior suggests that for x away from zero the dynamically calculated QCD distributions slightly underestimate the gluon and sea content of the hadrons. However, this is not too surprising in view of the fact that the calculation rests on the assumption[16] that at low resolution energies hadrons consist of valence quarks *alone*. Thus, this set of gluon and sea distributions represents one extreme while the flatter counting-rule distributions represent another. It is for this reason that the bands are shown in Figs. 8 and 9.

IV. CONCLUSIONS

The production of the J/ψ using different beams is a particularly sensitive probe of both quark and gluon distributions. When $\pi^{\pm}$ beams are used the x_F distribution for $x_F \gtrsim 0.5$ is particularly sensitive

to the behavior of the valence density $xv^{\pi}(x)$ as $x \to 1$. In particular, the rapid falloff observed in the data strongly favors a Farrar-type[19] (counting-rule) valence distribution for the pion as opposed to that form advocated by Field and Feynman.[17] The x_F dependence at sufficiently high energies and small x_F is sensitive to the gluon distribution. In particular, the pN data at small x_F require a dominant gluon contribution since the shape predicted by the $q\bar{q}$ mechanism alone is far too flat. The various total-cross-section beam ratios are also extremely sensitive to the gluon content of the hadrons. The results obtained here demonstrate the necessity of including *both* the $q\bar{q}$ *and* the gg fusion mechanisms in order to achieve agreement with recent CERN[13] and Fermilab[20] measurements. Since for increasing energies the gluon contribution rapidly increases, additional data at higher energies, especially with $\bar{p}$ and $K^{\pm}$ beams, are needed to test the predictions given by these mechanisms.

These results have demonstrated the importance of including gluon effects in hadron-hadron interactions. Therefore, the inclusion of these effects in other types of hadron production should be of comparable importance and cannot, henceforth, be neglected.

ACKNOWLEDGMENTS

One of us (E.R.) would like to thank H. Fritzsch for valuable discussions and is grateful to the members of the High Energy Physics Group at the Florida State University for their kind hospitality, as well as to the Freunde der Universität Mainz for financial support. The work of J.F.O. and E.R. was supported in part by the U.S. Energy Research and Development Administration.

APPENDIX

The cross section for gluons to produce a $c\bar{c}$ pair is determined from the Feynman diagrams of Fig. 4. Summing over final spins and colors and averaging over the initial ones yields the following differential cross section:

$$\frac{d\sigma^{gg\to c\bar{c}}}{dt}=\frac{\pi\alpha_s^{\,2}}{64s^2}\left(12M_{ss}+\tfrac{16}{3}M_{tt}+\tfrac{16}{3}M_{uu}+6M_{st}+6M_{su}-\tfrac{2}{3}M_{tu}\right), \tag{A1}$$

with

$$\begin{aligned}
M_{ss}&=\frac{4}{s^2}(t-m^2)(u-m^2),\\
M_{tt}&=\frac{-2}{(t-M^2)^2}\left[4m^4-(t-m^2)(u-m^2)+2m^2(t-m^2)\right],\\
M_{uu}&=\frac{-2}{(u-m^2)^2}\left[4m^4-(u-m^2)(t-m^2)+2m^2(u-m^2)\right],\\
M_{st}&=\frac{4}{s(t-m^2)}\left[m^4-t(s+t)\right],\\
M_{su}&=\frac{4}{s(u-m^2)}\left[m^4-u(s+u)\right],\\
M_{tu}&=\frac{-4m^2}{(t-m^2)(u-m^2)}\left[4m^2+(t-m^2)+(u-m^2)\right],
\end{aligned} \tag{A2}$$

and where the coefficients of these terms in the parentheses of Eq. (A1) are the appropriate color factors. The factor $\frac{1}{64}$ is due to averaging over the ingoing gluon octet colors. The invariants s,t,u are defined as usual and satisfy $s+t+u=2m^2$ where $m\equiv m_c$ is the mass of the charmed quark. Note that s here refers to the subprocess $gg\to c\bar{c}$ and should not be confused with $s=(p_A+p_B)^2$ in Eqs. (1) and (2), but should be identified with the Q^2 of Sec. II.

Integrating over

$$-\tfrac{1}{2}s-\tfrac{1}{2}[s(s-4m^2)]^{1/2}\leq t-m^2\leq -\tfrac{1}{2}s+\tfrac{1}{2}[s(s-4m^2)]^{1/2}, \tag{A3}$$

gives the total cross section

$$\sigma^{gg\to c\bar{c}}=\frac{\pi\alpha_s^{\,2}}{64s}\left[12(\tfrac{2}{3}+\tfrac{1}{3}\gamma)(1-\gamma)^{1/2}+\tfrac{16}{3}\left((4+2\gamma)\ln\frac{1+(1-\gamma)^{1/2}}{1-(1-\gamma)^{1/2}}-4(1+\gamma)(1-\gamma)^{1/2}\right)+6\left(2\gamma\ln\frac{1+(1-\gamma)^{1/2}}{1-(1-\gamma)^{1/2}}-4(1+\gamma)(1-\gamma)^{1/2}\right)-\tfrac{2}{3}2\gamma(1-\gamma)\ln\frac{1+(1-\gamma)^{1/2}}{1-(1-\gamma)^{1/2}}\right] \tag{A4}$$

with $\gamma\equiv 4m^2/s\leq 1$.

[1]J. J. Aubert *et al.*, Phys. Rev. Lett. 33, 1404 (1974).
[2]S. D. Drell and T. M. Yan, Phys. Rev. Lett. 25, 316 (1970); Ann. Phys. (N.Y.) 66, 578 (1971).
[3]J. F. Gunion, Phys. Rev. D 11, 1796 (1975); 12, 1345 (1975).
[4]M. B. Green, M. Jacob, and P. V. Landshoff, Nuovo Cimento 29A, 123 (1975).
[5]A. Donnachie and P. V. Landshoff, Nucl. Phys. B112, 233 (1976).
[6]D. Sivers, Nucl. Phys. B106, 95 (1976); E. Witten, *ibid.*

B104, 445 (1976); I. Hinchliffe and C. H. Llewellyn Smith, Phys. Lett. 66B, 281 (1977); A. J. Buras and K. J. F. Gaemers, Nucl. Phys. B132, 249 (1978).
[7]M. Glück and E. Reya, Phys. Rev. D 16, 3242 (1977).
[8]J. Steinberger, invited talk at the International EPS Conference held at Budapest, 1977 (unpublished); B. C. Barish *et al.*, Caltech Report No. CALT 68-606, 1977 (unpublished).
[9]H. L. Anderson *et al.*, Phys. Rev. Lett. 38, 1450 (1977).
[10]M. Glück and E. Reya, Phys. Lett. B (to be published).
[11]J. G. Branson *et al.*, Phys. Rev. Lett. 38, 580 (1977); 38, 791(E) (1977).
[12]H. Fritzsch, Phys. Lett. 67B, 217 (1977).
[13]M. J. Corden *et al.*, Phys. Lett. 68B, 96 (1977).
[14]M. B. Einhorn and S. D. Ellis, Phys. Rev. D 12, 2007 (1975).
[15]S. D. Ellis, M. B. Einhorn, and C. Quigg, Phys. Rev. Lett. 36, 1263 (1976); C. E. Carlson and R. Suaya, Phys. Rev. D 15, 1416 (1977).
[16]M. Glück and E. Reya, Nucl. Phys. B130, 76 (1977).
[17]R. D. Field and R. P. Feynman, Phys. Rev. D 15, 2590 (1977).
[18]V. Barger and R. J. N. Phillips, Nucl. Phys. B73, 269 (1974).
[19]G. R. Farrar, Nucl. Phys. B77, 429 (1974).
[20]J. G. Branson *et al.*, Phys. Rev. Lett. 38, 1331 (1977).
[21]Y. Kinoshita and K. Kinoshita, University of Bielefeld Report No. BI-TP 77/11, 1977 (unpublished).
[22]J. J. Aubert *et al.*, Nucl. Phys. B89, 1 (1975).
[23]Yu. M. Antipov *et al.*, Phys. Lett. 60B, 309 (1976).
[24]J. G. Branson *et al.*, Phys. Rev. Lett. 38, 1331 (1977); K. J. Anderson *et al.*, *ibid.* 37, 799 (1976). The errors shown were obtained from the parametrizations used to extrapolate $Ed\sigma/dx_F$ to $x_F = 0$.
[25]J. H. Cobb *et al.*, Phys. Lett. 68B, 101 (1977).
[26]H. D. Snyder *et al.*, Phys. Rev. Lett. 36, 1415 (1976).
[27]F. W. Büsser *et al.*, Phys. Lett. 56B, 482 (1975). The cross section has been increased by 60% corresponding to $\langle p_T \rangle_{\mu^+\mu^-} = 1$ GeV/c.
[28]E. Amaldi *et al.*, Lett. Nuovo Cimento 19, 152 (1977).